# A Study on Flexible Parallel Robots via Additive Manufacturing

Divya Shah[0000−0002−1246−5556] and Alberto Parmiggiani[0000−0003−1677−9381]

Centre for Robotics and Intelligent Systems (CRIS),
Istituto Italiano di Tecnologia (IIT), via S. Quirico 19/D,
Genova 16163, Italy https://www.iit.it
name.surname@iit.it

**Abstract.** The manufacturing and assembly of small parallel robots are often complex because of the required tolerances and high part count. The present work considers the use of compliant mechanisms to overcome some of these difficulties. Taking as a reference a recently published two degrees of freedom parallel orientational mechanism, we address several aspects related to the design and manufacturing of this type of small-scale systems. We consider two implementations of this mechanism, one developed following a "traditional" approach with linkages and pin joints, and one developed following a "flexible" approach using flexures. We then compare these two by providing qualitative and quantitative indications of their motion precision and capacity to withstand loads.

**Keywords:** Additive manufacturing · Parallel kinematics · Compliant mechanisms · Flexure hinges

## 1 Introduction

Parallel mechanisms and robots provide several advantageous properties such as greater rigidity, higher speeds, lesser sensitivity to input errors (see [3]), and synergistic behavior in load distribution, when compared to serial ones. These advantages generally come at the cost of mechanical complexity; the manufacturing and assembly of these mechanisms is thus quite challenging. Since parallel mechanisms comprise kinematic loops, their components need to mate with high precision, requiring tight tolerances, which are generally expensive. Moreover, only traditional CNC processes allow fabrication with these tolerances, that are otherwise difficult to obtain (e.g. when employing additive manufacturing (AM)).

Furthermore, tolerance selection is generally tricky, as the designer needs to strike the right balance between making an easily assemblable mechanism yet minimizing the overall amount of backlash. In this typical trade-off situation, the resulting system is likely to have either too much friction or too much backlash; if at all possible, finding the sweet spot is indeed difficult.

A possible solution to overcome this issue is to replace the joints of parallel robots with compliant joints, thus turning them into compliant mechanisms. This field has been widely studied in the past two decades: the books by Howell

[11,12] and Lobontiou [15] provide comprehensive overviews of as well as coverage of design approaches and guidelines along with several examples of compliant mechanisms and their applications.

The application of compliant mechanisms to robotic systems poses some interesting challenges. Indeed most robotic systems require relatively large ranges of motion which are difficult to obtain with compliant mechanisms whose strain directly affects their durability and robustness. It is, therefore, interesting to consider the solutions to this problem that are available in the literature.

Early implementations in mechatronic devices can be found in the work of Shimada et al.[25], that relied on cutting and folding of thin sheet metal plates.

Since the amount of strain obtained by the repeated bending of metal laminae was limited, the "cut-and-fold" approach was refined in the works of Fearing, Wood et al. with the adoption of laminated composites in a process dubbed "Smart Composite Microstructures" (SCM). The materials used for the flexible part of the joint were mainly Nylon and PET, while the rigid part was made in carbon fibre, fibreglass [26,10]but also stiff cardboard [21] and posterboard [8]. Researchers demonstrated that this approach is suitable for the fabrication of "micro-robots" and "meso-robots" with remarkable mobility. Recently the same approach has seen implementations in miniature robots for surgery [16] and haptics [22,18].

The work presented in the US20090260473A1 patent by Gosselin [7] is also reminiscent of SCM. In this case, Gosselin proposed obtaining the flexible element either with textile tapes or with properly arranged cables.

A different approach, adopted for example by Henein et al. [9], is to form metallic materials from bulk with Electric Discharge Machining (EDM). Naves et al. started from the "butterfly" hinge design by Henein et al. to develop the flexure-based suspension for an iron core direct drive torque motor with a range of motion of 60°[20]. Naves et al. also recently developed a spherical flexure joint having large stroke and high off-axis stiffness [19] with smartly arranged leaf springs. Both previous works were employed and integrated into a high precision hexapod robot.

A different approach to create flexible hinges is to locally tune the material properties of a structure. In Shape Deposition Manufacturing (SDM) and Hybrid Deposition Manufacturing (HDM) this is achieved through a multiple step moulding process that allows constructing flexure hinges by integrating viscoelastic parts within otherwise rigid structures. Robot legs [2] and underactuated robot hands [5] have, for example, been fabricated successfully with this technique.

Alternative approaches for constructing compliant joints with large displacements take advantage of the design freedom allowed by AM. Along these lines, interesting examples can be found in the work of Fowler et al. [6], that presents an evolution of the "butterfly-hinge" design by Henein et al., fabricated via additive manufacturing in titanium. Other interesting designs relying on AM can be found in the work of Merriam et al. [17] that presents the development of a 2DOF pointing mechanism for space applications and Kiener et al. [13]that

presents the construction of a flex type pivot with interlocked flexure blades and a compliant rotation reduction mechanism.

Our goal in the current work was to advance the state of the art of compliant robots fabricated in plastics via AM ([4]). Examples of the use of printed plastic parts are found in the work of Sharkey et al. [24] that presents a monolithic 3D printed flexure translation stage, that forms the key element of an open-source miniature microscope. The component was fabricated via Fused Filament Fabrication (FFF). Almeida et al. also present a 3D printed flexure-based robotic microtweezers device for precision manipulation [1] that is obtained with Selective Laser Sintering (SLS).

Compared to metal AM and metal EDM cutting, plastic AM is generally a more affordable and accessible process. Also, plastics are generally more tolerant to strain, making them an ideal choice for constructing compliant joints. Compared to SCM, plastic AM has the advantage of being less constrained to geometries to be obtained by folding, thus allowing a bit more design freedom for the development of vertical features. Finally, if compared to SDM and HDM, plastic AM has the advantage of being a simpler process, requiring neither moulds nor component curing, where the components can be fabricated in near net shape.

For these reasons, in this work, we started from a recent example of a 2DOF parallel orientational mechanism [14,23] constructed with a traditional approach and considered its fabrication instead via plastic AM.

## 2 Mechanism Description

The proposed 2 DOF parallel orientational mechanism, hereafter named *2DPOM*, is inspired by the idea of quaternion joint mechanism (as proposed in [14]), and is as shown in Fig. 1.

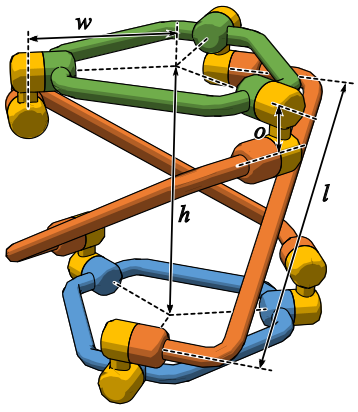


**Fig. 1.** Schematic representation of the proposed 2DPOM.

It has a kinematic architecture of three identical "legs" of two universal joints (coloured yellow), or equivalently four revolute joints, each diagonally connecting the fixed base (coloured blue) to the moving platform (coloured green). This arrangement achieves a structure similar to a three-dimensional anti-parallelogram and it emulates the rolling contact motion of two spheres.

The system geometry is fully determined with three independent parameters: $l$, $o$, and $w$. The parameter $l$ corresponds to the diagonal distance between inner axes of the universal joints of each leg. The parameter $o$ represents the offset between two axes of the universal joint. The parameter $w$ signifies the radial distance of the outer joint axes from the central axis of symmetry. Other dependent parameters include, the angle of inclination of the diagonal link with the axis of symmetry, $\alpha = \sin^{-1}(2w/l)$, and the total vertical distance between the outer two revolute joints, $h = \sqrt{l^2 - (2w)^2} + 2o$. Further details on the kinematics of the 2DPOM mechanisms are available in [14,23].

As a baseline for this study we used a 2DPOM mechanism constructed with a traditional approach. The geometric parameters were set to be $l = 45$[mm], $o = 6$[mm] and $w = 19$[mm]. This mechanism was assembled by putting together custom plastic parts and commercially available stainless steel guiding pins acting as bushings. The plastic parts were fabricated in Nylon (Polyamide 12) on a ProX SLS 6100 Selective Laser Sintering (SLS) additive manufacturing machine by 3D Systems.

## 3 Flexure Design

We were interested in geometries that could be obtained via AM, and more in detail with the Fused Filament Fabrication (FFF) manufacturing process, that is also referred to as Fused Deposition Modeling (FDM).

For this study we used the Markforged MarkTwo and Stratasys Fortus 400mc AM systems. We selected Nylon as a construction material among the available ones, because it had a low Young's Modulus (hence a good flexibility), and best resistance to stiffness ratio. These first experimentations led to the conclusion that the quality and durability of the flexure depends on the minimum layer thickness that can be obtained with each printer. The minimum layer thickness for the Markforged MarkTwo system is 0.1[mm], whereas that for the Stratasys Fortus 400mc system is 0.178[mm]. We thus decided to continue this study with the MarkTwo system.

We then designed an appropriate flexure geometry that was easy to obtain with such manufacturing process.

A first aspect that guided our design decisions was that bending flexures do not have a constant centre of rotation but we wanted to approximate rotational joints of the 2DPOM mechanism. For this reason we designed the flexures in our system to have the shortest possible flexure length. The selected flexure geometry is represented in Fig. 2.

A second aspect relates to FFF requiring the addition of supports for overhanging geometries. The addition of supports compromises the surface quality

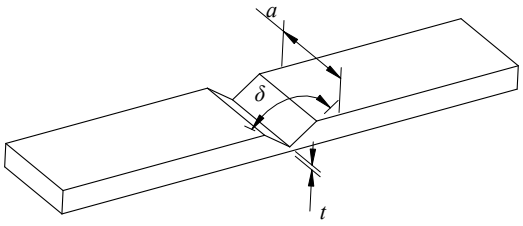


**Fig. 2.** Flexure geometry. The figure shows the selected flexure geometry with its main parameters being flexure width ($a$), flexure thickness ($t$) and the notch angle($\delta$).

where the supports meet the part; this must be avoided in the flexure region to guarantee the highest fatigue life for the mechanism.

The build strategy for the flexure is represented in detail in Fig. 3.

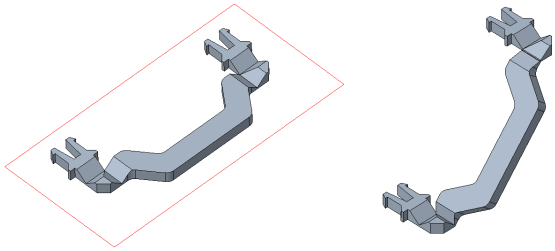


**Fig. 3.** "Leg manufacturing". The figure represents one of the three support "legs" of the mechanism. To ensure the maximum flexure resistance all flexure axes shall be parallel to the build plane at the manufacturing stage (a). Once each "leg" has been manufactured, it is assembled in the mechanism's neutral configuration (b). This, however, pre-strains the two inner flexures of each "leg" which are not at zero strain in the mechanism's neutral configuration.

In the region of the flexures we set the slicer parameters so as to align the paths of the FFF extruder perpendicularly to the flexure (Fig. 4). This results in a joint that is structurally rather similar to the solutions proposed in the US20090260473A1 patent by Gosselin [7], where very short and compact flexures were obtained with textiles and cables. The main difference in our case is that the short bending structures were fabricated with the same material as of the rigid structural parts (Nylon).

An unwanted side-effect of using Nylon is that the printed part remains very flexible also during the print process, and tends to curl and detach from the printer bed, especially on large builds when the part has time to cool. To avoid this issue parts having thin sections were printed with the "brim" option

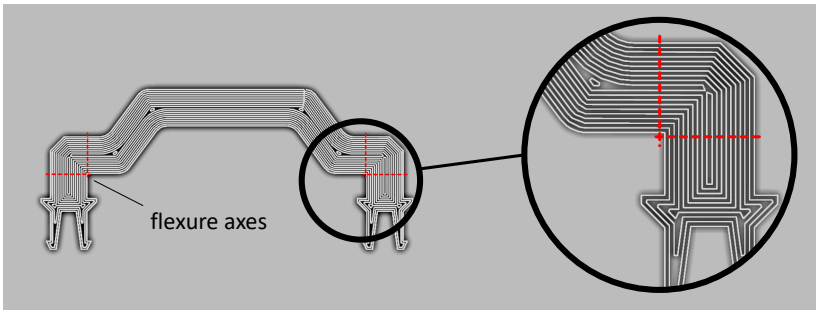


**Fig. 4.** Extruder paths on flexure plane. The figure shows the paths followed by the FFF extruder to deposit the fused plastic filament. The paths were designed to cross the flexures perpendicularly to their rotation axis on all flexure layers, so as to maximize the flexures' resistance to bending.

activated: in this case a series of contours are printed around the actual part to improve its adhesion to the print bed.

The initial design was subsequently optimized iteratively by building physical prototypes and subjecting them to the motions they would experience when integrated in the 2DPOM mechanism. The final design of the flexures in this study had a flexure thickness $t$ of 0.5[mm], a flexure width $a$ of 4.0[mm] and a notch angle $\delta$ of 100°.

Figure 5 compares CAD render and the real prototypes for both the traditional and flexible mechanisms.

(a) (b)

**Fig. 5.** Mechanism comparison. The figure presents a CAD view (a) and a photograph (b) of the two implementations of the 2DPOM mechanism considered for this work. The "traditional" design is represented on the left, while the "flexible" design on the right in both sub-figures. In (a) corresponding parts are represented with the same colours. As can be seen, the flexure-based design is considerably simpler being made with five parts instead of eleven (connection pins excluded).

# 4 Experimental Validation

## 4.1 Backlash assessment

To assess the backlash within both mechanisms, we subjected them to a particular actuator trajectory multiple times and observed the corresponding platform motions for each repetition. One of the actuator was moved form zero configuration to maximum limit in one direction and back. This also corresponds to the platform reaching the maximum tilt and back, while keeping the azimuth constant. We repeated this motion five times.

Since this kinematic architecture lacks a fixed instantaneous center of rotation, measuring the platform orientations directly is not straightforward. Hence, for this experiment we used external sensors in the form of a motion capture system. More in detail we employed a Vicon Vantage motion tracking system with Vicon Nexus data capture software, having an accuracy of 0.017[mm] with root mean squared error value of 0.324[mm]. We attached markers at specific locations on the base and the platform so as to track their positions for the entire motion. We then extracted the platform orientations from the motion capture data following the Tilt & Torsion paramterization ([23]).

Figure 6, shows the resulting platform orientations, expressed in polar coordinates ($r$, $\theta$). The tilt corresponds to the radius ($r$) of the plot where as the azimuth is the angle ($\theta$). It can be observed that the readings for the mechanism fabricated with traditional approach are more scattered as compared to the flexible version. We interpret this observation as the flexible model having higher precision than the traditional one. In other words, the traditional model shows higher backlash as compared to the flexible one.

## 4.2 Loading test

We subsequently performed a loading test of the two mechanisms to provide a qualitative representation of their response under load. Both mechanisms were compressed, in their zero configuration, with a Zwick-Roell ProLine Z050/TN BT1-FB050TN.D30 testing machine (see Fig.7(c)). The mechanisms were first compressed gradually to 30[N] with a cross-bar speed of 5[mm/min]; this test was repeated five times in each condition. The force-displacement characteristic curves of the two versions of the mechanism are shown in Fig.7(a). Despite its flexures the compliant mechanism results being stiffer, because its geometry allows constructing it with a lower $\alpha$ angle. At approximately 8.5[mm] of displacement, the mechanism fabricated with the traditional approach deflected until its links self-collided: further loading was deemed unnecessary. The flexure based mechanism was instead loaded until failure. The result of this test are shown in Fig.7(b). As can be seen the flexible version of mechanism can withstand up to 70[N] before failing. Failure occurs at the first flexure (Fig.7(d)), that in the zero-configuration is subject to torsional loading.

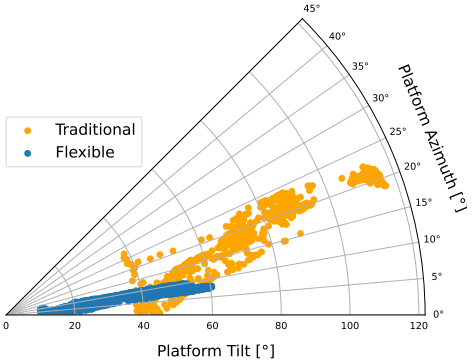


**Fig. 6.** Backlash assessment. Figure represents comparison of the platform motion (azimuth and tilt) between the traditional and flexible mechanism models, expressed in polar coordinates.

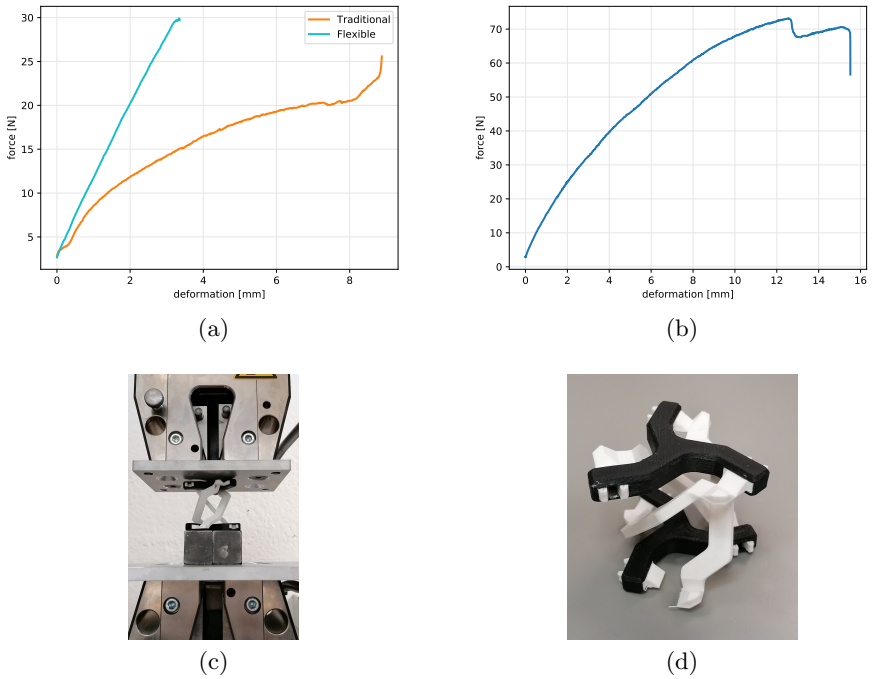


**Fig. 7.** Load testing. The figure shows results of the loading tests in (a) and (b). Subfigure (a) compares the response under load of the traditional and flexible mechanisms. Each curve represents the average of five repetitions of the loading test. The graph in (b) represents the force-displacement curve of the flexible mechanism when loaded until failure. The loading test setup is shown in (c); the failure of the flexure-based version is shown in (d).

## 5 Conclusions

The experiments shown in this work show how Nylon (Polyammide12) is a suitable material that allows the construction of flexure hinges with large displacements. Further work shall be carried out to better characterize the flexures' fatigue life as a function of the applied loads and the number of loading cycles. The adoption of AM implies manufacturing constraints on the flexure geometry; how these aspects can be dealt with at the design stage shall also be characterized more in detail. Nevertheless, the approach is promising because the robots made in this way are less subject to mechanical backlash and are easier to construct and assemble being made from fewer parts. Therefore, we think the results presented in the current work further confirm how FFF can be considered a practical technology for fabricating small-scale flexible parallel robots.

## References

1. Almeida, A., Andrews, G., Jaiswal, D., Hoshino, K.: The Actuation Mechanism of 3D Printed Flexure-Based Robotic Microtweezers. Micromachines **10**(7), 470 (Jul 2019). https://doi.org/10.3390/mi10070470
2. Bailey, S., Cham, J., Cutkosky, M., Full, R.: Biomimetic robotic mechanisms via shape deposition manufacturing. Robotics Research: The Ninth International Symposium (Jan 2000)
3. Briot, S., Bonev, I.A.: ARE PARALLEL ROBOTS MORE ACCURATE THAN SERIAL ROBOTS? Transactions of the Canadian Society for Mechanical Engineering **31**(4), 445–455 (Dec 2007). https://doi.org/10.1139/tcsme-2007-0032
4. Calignano, F., Manfredi, D., Ambrosio, E.P., Biamino, S., Lombardi, M., Atzeni, E., Salmi, A., Minetola, P., Iuliano, L., Fino, P.: Overview on Additive Manufacturing Technologies. Proceedings of the IEEE **105**(4), 593–612 (Apr 2017). https://doi.org/10.1109/JPROC.2016.2625098
5. Dollar, A.M., Howe, R.D.: A robust compliant grasper via shape deposition manufacturing. IEEE/ASME Transactions on Mechatronics **11**(2), 154–161 (2006). https://doi.org/10.1109/TMECH.2006.871090
6. Fowler, R.M., Maselli, A., Pluimers, P., Magleby, S.P., Howell, L.L.: Flex-16: A large-displacement monolithic compliant rotational hinge. Mechanism and Machine Theory **82**, 203–217 (Dec 2014). https://doi.org/10.1016/j.mechmachtheory.2014.08.008
7. Gosselin, F.: Jointed limb comprising fibres, and jointed structure and robot or haptic interface comprising such a jointed limb (Oct 2009), https://patents.google.com/patent/US20090260473A1/en
8. Haldane, D.W., Peterson, K.C., Garcia Bermudez, F.L., Fearing, R.S.: Animal-inspired design and aerodynamic stabilization of a hexapedal millirobot. In: IEEE Int. Conf. on Robotics and Automation (ICRA). pp. 3279–3286 (2013). https://doi.org/10.1109/ICRA.2013.6631034
9. Henein, S., Spanoudakis, P., Droz, S., Myklebust, L.I., Onillon, E.: Flexure pivot for aerospace mechanisms. In: 10th European Space Mechanisms and Tribology Symposium. pp. 285–288. Citeseer (2003)
10. Hoover, A.M., Fearing, R.S.: Fast scale prototyping for folded millirobots. In: IEEE Int. Conf. on Robotics and Automation (ICRA). pp. 886–892. IEEE (May 2008). https://doi.org/10.1109/ROBOT.2008.4543317

11. Howell, L.L.: Compliant Mechanisms. Wiley-Interscience (Aug 2001)
12. Howell, L.L., Magleby, S.P., Olsen, B.M., Wiley, J.: Handbook of compliant mechanisms. Wiley Online Library (Feb 2013). https://doi.org/10.1002/9781118516485
13. Kiener, L., Saudan, H., Cosandier, F., Perruchoud, G., Spanoudakis, P.: Innovative concept of compliant mechanisms made by additive manufacturing. MATEC Web of Conferences **304**, 07002 (Jan 2019). https://doi.org/10.1051/matecconf/201930407002
14. Kim, Y.J., Kim, J.I., Jang, W.: Quaternion Joint: Dexterous 3-DOF Joint representing quaternion motion for high-speed safe interaction. In: IEEE/RSJ Int. Conf on Intelligent Robots and Systems (IROS). pp. 935–942. IEEE (Oct 2018). https://doi.org/10.1109/IROS.2018.8594301
15. Lobontiu, N.: Compliant Mechanisms: Design of Flexure Hinges. CRC Press (Dec 2002)
16. McClintock, H., Temel, F.Z., Doshi, N., Koh, J.s., Wood, R.J.: The milliDelta: A high-bandwidth, high-precision, millimeter-scale delta robot. Science Robotics **3**(14) (Jan 2018). https://doi.org/10.1126/scirobotics.aar3018
17. Merriam, E.G., Jones, J.E., Magleby, S.P., Howell, L.L.: Monolithic 2 dof fully compliant space pointing mechanism. Mechanical Sciences **4**(2), 381–390 (2013). https://doi.org/10.5194/ms-4-381-2013
18. Mintchev, S., Salerno, M., Cherpillod, A., Scaduto, S., Paik, J.: A portable three-degrees-of-freedom force feedback origami robot for human–robot interactions. Nature Machine Intelligence **1**(12), 584–593 (Dec 2019). https://doi.org/10.1038/s42256-019-0125-1
19. Naves, M., Aarts, R., Brouwer, D.: Large stroke high off-axis stiffness three degree of freedom spherical flexure joint. Precision engineering **56**, 422–431 (Mar 2019). https://doi.org/10.1016/j.precisioneng.2019.01.011
20. Naves, M., Nijenhuis, M., Hakvoort, W., Brouwer, D.: Flexure-based 60 degrees stroke actuator suspension for a high torque iron core motor. Precision engineering **63**, 105–114 (May 2020). https://doi.org/10.1016/j.precisioneng.2020.02.001
21. Pullin, A.O., Kohut, N.J., Zarrouk, D., Fearing, R.S.: Dynamic turning of 13 cm robot comparing tail and differential drive. In: IEEE Int. Conf. on Robotics and Automation (ICRA). pp. 5086–5093 (2012). https://doi.org/10.1109/ICRA.2012.6225261
22. Salerno, M., Zhang, K., Menciassi, A., Dai, J.S.: A novel 4-DOF origami grasper with an SMA-actuation system for minimally invasive surgery. IEEE Transactions on Robotics **32**(3), 484–498 (Apr 2016). https://doi.org/10.1109/TRO.2016.2539373
23. Shah, D., Wu, Y., Scalzo, A., Metta, G., Parmiggiani, A.: A comparison of robot wrist implementations for the iCub humanoid. Robotics **8**(1), 11 (Feb 2019). https://doi.org/10.3390/robotics8010011
24. Sharkey, J.P., Foo, D.C.W., Kabla, A., Baumberg, J.J., Bowman, R.W.: A one-piece 3D printed flexure translation stage for open-source microscopy. Review of Scientific Instruments **87**(2), 025104 (Feb 2016). https://doi.org/10.1063/1.4941068
25. Shimada, E., Thompson, J., Yan, J., Wood, R., Fearing, R.: Prototyping millirobots using dextrous microassembly and folding. Proc. ASME IMECE/DSCD **69**(2), 933–940 (2000)
26. Wood, R.J., Avadhanula, S., Menon, M., Fearing, R.S.: Microrobotics using composite materials: The micromechanical flying insect thorax. In: IEEE Int. Conf. on Robotics and Automation (ICRA). vol. 2, pp. 1842–1849. IEEE (Sep 2003). https://doi.org/10.1109/ROBOT.2003.1241863